Comparison of V-shaped IPM Machines Winding Topologies for Heavy-duty EV Applications

Leia George, Adam Walker, Fengyu Zhang, Gaurang Vakil, Chris Gerada
Power Electronics Machines and Control Group
University of Nottingham
Nottingham, UK
eeylg1@nottingham.ac.uk

***Abstract*—High performance electric machines are critical for heavy-duty electric vehicles (HDEV) to enable transportation electrification, where there is a significant performance gap between the traditional internal combustion engines and electrical machine technology. Winding topologies are critical in the design of electrical machines, the developments of which are widely reported in other applications such as automotives, but rarely studied for HDEV applications. This paper will provide a detailed review to assess both widely used and novel winding characteristics in HDEV. Using an 8000RPM, 370kW, interior, V-shaped permanent magnet (PM) machine case study, various winding designs are compared. An evaluation method has been proposed to provide a comprehensive review of each winding topologies' effects on machine performance.**

Keywords—Winding design, HDEV, comparison, simulation

I. INTRODUCTION

Well established environmental concerns have resulted in a collective move towards clean transportation solutions. This has resulted in heavy research interest in the electrification of passenger electric vehicles (EVs) and appropriate infrastructure to accommodate them. Research into the technological requirements to deliver on these goals has reached a level of confidence, with all combustion-based vehicles to be phased out from 2025, globally [1].

Due to disproportionate amounts of CO_2/km produced, heavy-duty electric vehicles (HDEVs) have attracted more attention, leading to interest in motor solutions capable of high torque density and efficiency over a wide-speed range. HDEVs are a research challenge as high-power density and fault-tolerant requirements push thermal and mechanical limits, such as rotor peripheral speed, meaning that multi-perspective design is needed [2].

The current availability of these solutions is highly limited, for example, the pre-production Tesla Semi is a class 8 electric vehicle comprised of four passenger EV motors, and these are not yet available [3]. Research surrounding HDEVs focuses on Permanent magnet (PM) topologies where winding topology choice is key to achieving high material utilisation, for power density and quality. Progress with these design aspects is a key contributor to achievement of HDEV motor solutions [4].

This paper looks at winding topologies available in current literature, followed by simulation comparisons on a 370kW baseline machine. Section II presents different topologies compared on the baseline machine, followed by slot considerations and evaluation in Section III, end winding considerations in section IV and connection considerations in section V. Finally, Section VI concludes the research.

II. BASELINE MACHINE

The winding topologies to be considered in this paper are shown in Fig.1, which illustrates the procedure used in winding topology construction A baseline machine is used to compare the aforementioned winding topologies.

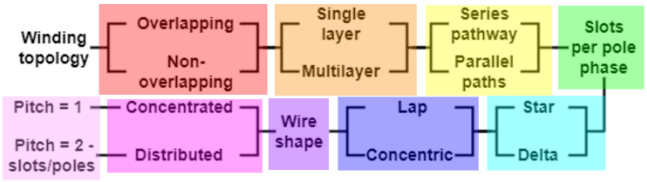

Fig. 1. Winding topology classification process

The baseline machine requirement is listed in Table I. It is an 8000RPM, 370kW, permanent magnet (PM) machine with an interior, V-shaped PM layout. In general, the machine volume and electrical inputs parameters are fixed with power as the comparative output parameter. The rotor pole number varies (4 or 6) with constant PM mass

TABLE I. BASELINE MACHINE PARAMETERS

Power	kW	370	Variable
Base Speed	rpm	8000	Fixed
RMS current	A	440	Fixed
Voltage	V	328	Limited
Slot/pole		36/6	Variable
Stator outer diameter	Mm	470	Fixed
Active length	mm	220	Fixed

Dual-three phase systems are commonly used for EVs due to increased fault tolerance [5] and are mainly considered for HDEV. Compared to single-three phase machines, dual-three phase systems can reduce the strain on power electronic systems with the reduction on individual converter requirements, i.e., two converters at 440A are easier to be implemented than one at 880A.

A baseline machine radial review is shown in Fig. 2 and the output data is shown in Table II, including torque/power density, torque per volt (TPV), efficiency, etc.. Housing water jacket cooling is applied which provides 70 L/min of 50/50 Ethylene-Glycol and water with inlet temperature at 65°. The drive characteristics will be used to design and optimise the baseline machine to meet the Advanced Propulsion Centre (APC) 2035 targets [6].

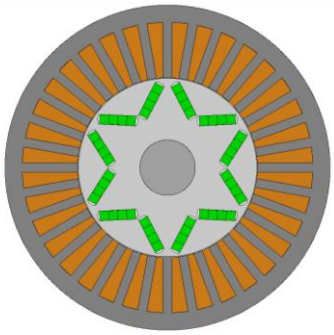

Fig. 2. Baseline machine radial diagram

TABLE II. BASELINE MACHINE OUTPUT DATA

Parameters	Unit	Baseline machine	APC 2035 targets
Torque density	Nm/kg	3.66	-
Power density	kW/kg	5.36	10
Efficiency	%	97.75	97
Average Winding temperature	°C	170.1	200
Torque ripple	%	75.2	5

III. SLOT CONSIDERATIONS

In this section, various winding types will be compared for the baseline machine in section II, mainly on the slot considerations.

A. *Overlapping/nonoverlapping*

Fig. 3 shows the overlapping windings (OLPW) and non-overlapping windings (NOLPW). For OLPW, the conductors are wrapped around the stator poles such that the end windings of different phases overlay each other [7]. This configuration tends to suffer from large torque ripple magnitudes, long end windings and higher winding temperatures [8].

For non-overlapping windings (NOLPW), conductors are wound around each pole independently and energized in different directions that do not overlay, which helps to increase fault tolerance for HDEV applications with smaller mutual inductance between phases, as these are physically and thermally insulated [2]. This contributes to lower temperature dependent losses such as current loss; however, magnetic losses may increase due to higher Magnetomotive force (MMF) harmonics in the airgap [9].

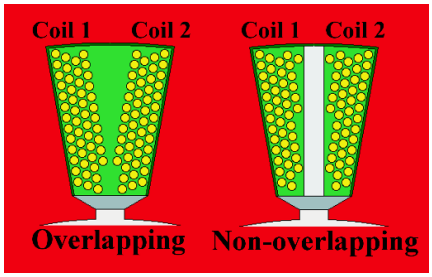

Fig. 3. Overlapping vs nonoverlapping diagram

The losses for the winding topologies are compared with an air divider added to the NOLPW, shown in Table III for two rotational speeds, rated rotational speed and max application speed to enter the field-weakening (FW) region. It can be seen that iron loss is the dominant loss source for both cases. However, the DC copper loss continues to separate the configurations from each other, leading to the differences in efficiency seen. The NOLPW has lower DC losses (4.5%) with reduced eddy current circulating in the slots due to the insulative effect that the air separator provides with low permeability and conductivity. The reason for the difference in efficiency is that the OLPW has higher amplitudes of harmonic content, contributing to distortion of the characteristics which cause increased copper loss. NOLPW does not have this due to physical separation between phases reducing distortion in voltage characteristics. From a manufacturing perspective, the construction of NOLPW is easier as the end windings do not overlap.

TABLE III. OVERLAPPING AND NONOVERLAPPING LOSSES

Parameter	8kRPM		20kRPM	
	OLPW	***NOLPW***	***OLPW***	***NOLPW***
Efficiency (%)	97.37	97.41	96.50	96.52
DC copper loss (kW)	3.34	3.15	4.51	4.13
AC copper loss (kW)	1.130	1.158	3.343	3.479
Iron loss (kW)	4.88	4.88	19.02	20.67

For OLPW, the distortion is higher for drive characteristics and geometric properties, such as cogging torque. This difference in cogging torque is an additional contributor to the increase in torque ripple for OLPW. Other key performance indicators such as torque density and power density are compared in Table IV which shows that the variation is insignificant (less than 1%) apart from temperature differences. These trends are consistent for high-speed operation including AC loss and the OLPW/NOLPW appear to have minimal impact on potential for FW.

TABLE IV. OLPW AND NOLPW COMPARISON

	T. dens (Nm/kg)	***P. dens (kW/kg)***	***TPV (Nm/V)***	***Eff. (%)***	***Temp (°C)***	***T. rip (%)***
OLPW	3.66	5.36	2.29	97.75	170.1	75.2
NOLPW	3.66	5.35	2.28	97.78	160.85	75.10
Change (%)	-0.193	-0.207	-0.244	+0.036	-4.993	-0.138

B. *Single/multi-layered*

The number of winding layers is also investigated in this paper. For a single layer winding (SLW), the coil number is half the number of stator slots and can be shown as each slot only having windings from a single phase. The number of coils to number of slots are equal for a double layer winding (DLW) and can be physically characterised by having two phases present in each slot, with stranded wire configurations typically being limited to two winding layers [10]. Shorter end windings, lower back electromotive force (BEMF) harmonics and reduced eddy current loss are shown for multilayer windings [11].

As shown in Fig. 4, the high order harmonic amplitude is larger for SLW because multilayer configurations utilize the harmonic spectra to enhance higher order harmonic suppression. The slots will typically contain two or more

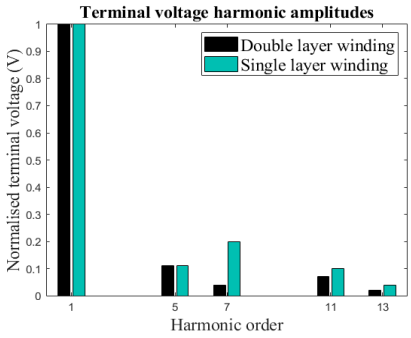

Fig. 4. Terminal voltage distortion for single and double layer windings

phases, each inducing BEMF that acts to increase or reduce harmonics. This is also true for air gap flux density; both BEMF harmonic suppression and air gap flux density harmonic suppression contribute to lower torque ripple.

Due to the slightly higher saliency ratio of the geometry (1.73 to 1.707) for the DLW, more cogging torque will be generated as well as higher torque over a larger speed range, which shows the enhanced FW potential. DLWs have higher efficiency because the increase in loss and temperature is larger for the SLW. To achieve comparable slot fill, the copper area per phase in the SLW is increased. This means phase resistance is lower for equivalent voltage, inducing higher eddy current loss in the iron, giving a ~14% temperature increase for the same electrical loading. As summarized in Table V, the SLW can achieve high torque amplitudes, but the DLW can deliver higher torque density over a larger speed range with FW, indicating suitability for HDEV applications.

TABLE V. SINGLE TO MULTILAYER COMPARISON

	T. dens (Nm/kg)	*P. dens (kW/kg)*	*TPV (Nm/V)*	*Eff. (%)*	*Temp (°C)*	*T. rip (%)*
SLW	3.63	5.23	2.23	97.37	196.60	74.64
DLW	3.66	5.36	2.29	97.75	170.10	75.20
Change(%)	+1.01	+2.50	+2.39	+0.38	-13.54	+0.74

C. Integer/fractional slot

Windings can be characterized as integer or fractional slot. An integer slot winding (ISW) has a whole number of slots per pole phase (SPP) whereas the fractional slot winding (FSW) has a non-integer number of SPP [12]. FSWs are shown to have better field weakening potential and shorter end windings [13] but also experiences larger harmonic content which causes increased losses [14]. Considered here for FSW are SPP = 0.5, 1.5, and 2.5

When augmenting from ISW to FSW, torque amplitude decreases as the periodicity of the machine is reduced due to the smaller Greatest Common Divisor (GCD) between slots and poles. This means that the harmonic content is reduced, and the maximum torque is therefore reduced [15]. Additionally, the end windings are shorter, decreasing the mass but not sufficiently to match the torque decrease, so FSW torque density is lower. Output distortion varies between FSWs as shown in Fig. 5 which shows reduced cogging torque with higher SPP due to the reduced GCD, that increases the cogging torque frequency and reduces amplitude. Torque ripple shares the same tendency with SPP, in that lower SPP corresponds to higher torque ripple, due to increased cogging torque as well as large harmonic distortion. This is reflected particularly by the 3 SPP case, which has very low distortion due to the high slot number which reduces distortion amplitude.

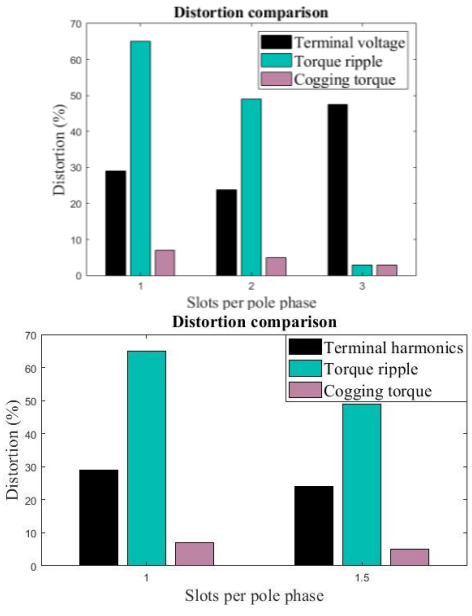

Fig. 5. Distortion characteristics for various slots per pole phase

On the contrary, the highest terminal distortion is observed for SPP2.5. SPP0.5 has high efficiency with low DC copper loss due to shorter end-windings, compared to SPP>1.5. However, the increase in slot number for SPP>1.5 does not necessarily reduce end-windings as overall winding mass is increasing. However, all FSWs showed improved temperature performance due to the reduced overlap of winding materials, which allows for improved cooling. The 0.5SPP winding has the highest saliency ratio, which is reflected by the torque-speed relationship. For SPP>1, the saliency ratio and potential FW region is reduced as the phases are not separated. Illustrated in Table VI, generally FSWs benefit from low temperatures and low distortion but ISWs have high density and efficiency.

TABLE VI. ISW AND FSW COMPARISON

	T. dens (Nm/kg)	*P. dens (kW/kg)*	*TPV (Nm/kg)*	*Eff. (%)*	*Temp (°C)*	*T. rip (%)*
ISW	2.29	2.36	1.21	94.62	301.60	65.33
FSW	1.76	2.30	1.23	93.70	278.25	49.28
Change (%)	-29.95	-2.62	+1.92	-0.99	-9.50	-32.57

D. Wire shapes

Wire type significantly affects the maximum slot fill factor that can be achieved for the machine, which changes the machine losses and thus machine efficiency. The following are some common wire types using in existing literature, with two types investigated on the baseline machine.

Conductors with a round cross-sectional area tend to be used in stranded configurations, these have inherently lower fill factor as there is unused space between the wires in the slot. Utilization when using round, stranded wires is limited to around 0.5 [13].

Bar conductors use a square or rectangular cross-sectional area. As the cross-sectional area is bigger, AC performance needs to be assessed to ensure performance at high speeds [16]. Material costs are higher, but manufacturing costs are lower, and robustness is improved by material strength and elimination of random gaps which cause vibrations [17]. It is found that hybrid rectangular wire wave windings that use both copper and aluminium can suppress eddy current loss induced by increased resistance [18].

Hairpin conductors are rectangular conductors in which the end windings are arranged such that they are not overlapping [13] which has the advantage of a scalable manufacturing process [19]. As with aforementioned rectangular wires, the fill factor and efficiency are improved with hairpin conductors, however large cross-sectional area means that AC skin effects and thermal hotspot management needs to be considered in design to minimize material degradation and failure [20].

Litz wire winding is made up of multiple, individually insulated strands connected in parallel and twisted together [21] to minimize AC loss in particular for high frequency operation. Design of these windings, however, can be difficult as these wire types are highly affected by AC proximity loss so high-quality loss evaluations are required [22]

Only the circular/stranded and rectangular/hairpin are considered at this stage in the paper. The inherently higher slot fill capability of hairpin conductors provides low DC losses for the hairpin winding, and thus gives higher machine efficiency. However, the hairpin conductors are heavier, showing a decrease in torque density in Table VII but improved temperature performance. The hairpin winding also

has higher D-axis inductance (83.01µH to 8.112µH) due to the influence of geometry such as cross-sectional area, length, and separation between turns [23]. This leads to higher saliency ratio, which contributes to larger FW region, as seen in Fig. 6. The torque-speed graphs show the comparison of the performance envelopes due to the application limited voltage and current, this region would be reduced in practice due to thermal and mechanical constraints.

A summary of these results moving from stranded to hairpin is given by Table VII, showing that more specialized wire shapes can have performance benefits but have costs in terms of ripple and system mass.

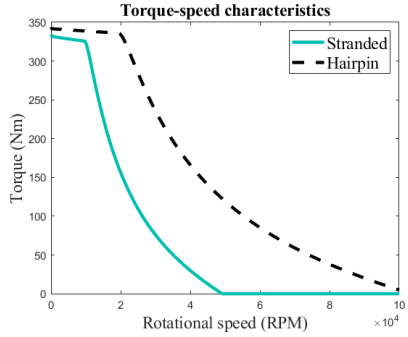

Fig. 6. Torque-speed comparison for wire types

TABLE VII. STRANDED TO HAIRPIN WIRE COMPARISON

	T. dens (Nm/kg)	*P. dens (kW/kg)*	*TPV (Nm/V)*	*Eff. (%)*	*Temp (°C)*	*T. rip (%)*
Stranded	2.58	5.25	2.28	95.00	248.75	68.95
Hairpin	2.22	4.52	2.36	96.46	180.35	78.82
Change (%)	-16.08	-16.13	3.44	+1.51	-35.21	+12.52

IV. END WINDING CONSIDERATIONS

A. *Lap/concentric*

The winding layout can be lap or concentric depending on how the coils are wound. Concentric windings have stacked coils whereas lap windings have overlapping coils for maximum flux linkage [24]. Concentric winding manufacturing processes are easier as automated winding techniques can be used, while it is challenging for lap as coil sides cannot be fitted to the slot until finishing coils are added [18].

The simulation data showed that most differences between the lap and concentric windings were small and aligned with literature as shown in Table VIII, such as minor BEMF amplitude differences [19].

TABLE VIII. LAP TO CONCENTRIC WINDING COMPARISON

	T. dens (Nm/kg)	*P. dens (kW/kg)*	*TPV (Nm/V)*	*Eff. (%)*	*Temp (°C)*	*T. rip (%)*
Lap	3.66	5.36	2.29	97.75	170.10	75.20
Con	3.66	5.36	2.29	97.75	170.10	75.20
Change (%)	+0.002	+0.002	+0.002	0.000	0.000	+0.003

B. *Pitch*

Windings can also be defined as full pitch (FPW) which has a coil pitch equal to the pole pitch or as short pitch (SPW) where the coil pitch is less than the pole span [12]. Related to this are concentrated windings (CW), which have a coil around each tooth, meaning that these are SPW with a coil throw of one slot. Similarly, distributed windings (DW) have coils that span multiple teeth, so can be FPW or SPW [25]. Fig. 7 illustrates the pole span and potential coil span; the pitch length is described as slots spanned by the coil/slots in pole span.

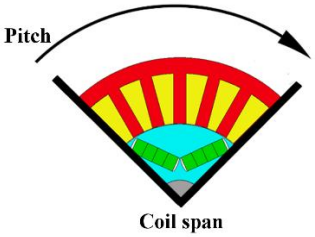

Fig. 7. Pole span coil span radial diagram

When comparing CW to DW, higher torque density, decreased power factor and lower efficiency are observed. Moreover, distortion in the CW is higher, with high harmonic content in the MMF leading to higher torque ripple and higher iron losses, this holds true for SPW [26]. Conversely, FPW has higher material costs due to the increase in copper mass with reduced losses, particularly eddy current loss in the iron [27].

Due to lower saliency ratio, lower reluctance torque is produced for CWs, this is a result of lower D-axis inductance for CWs. However, due to the shorter end windings, the overall winding mass and machine mass is smaller thus torque density is higher, as seen in Table IX. CW's dominant loss source is iron loss, particularly in the rotor, the losses are not proportionate to the output power hence the lower efficiency. Fig. 8 shows improved FW capability for CWs.

Pitch length has a pronounced effect on terminal distortion, which is lowest for 4/6 pitch. Further increase in pitch length does not reduce torque ripple due to the reduced cogging torque for low saliency i.e., long-pitched designs. The reduced saliency as pitch length increases means that the SPW 2/6 has largest FW region. Increasing pitch length reduces speed and increases torque, however, increasing pitch length also increases weight so the maximum torque density solution occurs at SPW 4/6.

Efficiency improves as pitch length increases due to reduction of parasitic effects of distortion, but phase resistance increases with pitch length, increasing phase voltage, DC copper loss and temperature dependent loss resulting in maximum efficiency at SPW 2/6. Generally, SPWs have improved power density and efficiency but FPWs have improved distortion.

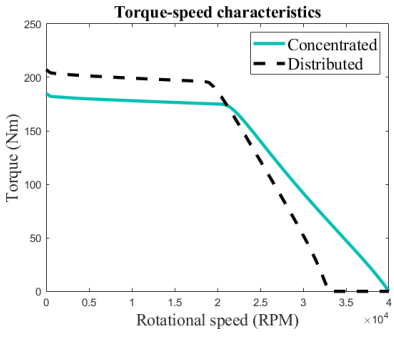

Fig. 8. Torque-speed characteristic comparison for concentrated and distributed windings

TABLE IX. VARIATION OF PITCH LENGTH

	T. dens (Nm/kg)	*P. dens (kW/kg)*	*TPV (Nm/V)*	*Eff. (%)*	*Temp (°C)*	*T. rip (%)*
CW	1.70	3.97	1.38	93.57	200.25	90.62
DW– SPW	3.83	2.72	1.15	95.23	353.80	44.00
DW- FPW	3.92	1.17	0.69	93.64	575.05	28.47

V. Connection Considerations

A. Star/delta

Winding input connections can be star or delta based. In star windings, coil ends are connected to a common neutral whereas for delta windings coils are joined end-to-end creating a closed loop. It is shown that star performance is better under healthy conditions, but delta is suited to open-phase faults due to the lower line resistance [28]. The combined star-delta windings have large potential benefits but are challenging to manufacture [24].

As seen in Table X, the differences between the winding configurations are not significant to the parameters considered for this application. Additionally, the usage of star and delta winding connections including performance and potential benefits is well reviewed in literature [29]. However, it is noteworthy that most expected benefits of changes between these input connections relate to manufacturing techniques and overall reliability, which are not considered at this stage.

TABLE X. Star to Delta Winding Input Comparison

	T. dens (Nm/kg)	*P. dens (kW/kg)*	*TPV (Nm/V)*	*Eff. (%)*	*Temp (°C)*	*T. rip (%)*
Star	3.66	3.07	2.29	97.75	170.10	75.20
Delta	3.66	3.07	2.29	97.75	170.10	75.20

B. Parallel paths

When coils are connected in series, current is not split between the coils, so electrical loading is increased. This is particularly problematic in anisotropic machines as the changes in permeability with mechanical rotation increase reluctance and cogging torque [30]. Connecting windings with parallel branches reduces winding cross-sectional area, reducing the loss and better adheres to voltage limits, particularly when the operational frequency is high, as the phase voltage is a function of frequency [31]. Usage of parallel paths can reduce impacts of permeability changes and unbalanced flux density [30], but complexity is increased so manufacture can be difficult [32].

Increasing parallel paths reduces the phase voltage by reducing series turns per coil and electrical loading. As electrical loading is reduced, temperatures in the three-path winding are smaller, which leads to improved efficiency with lower losses. Increasing parallel paths also decreases torque amplitude but increases speed disproportionately so the output power and power density is increased while the torque density is decreased. The two-path winding has higher torque amplitude with lower cogging torque as the three-path design has higher saliency, contributing higher cogging torque and larger FW region, illustrated in Fig. 9.

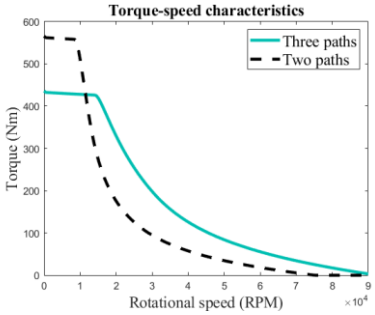

Fig. 9. Torque-speed characteristics for varying parallel path numbers

VI. Comparison of Winding Topologies

A scoring system will be proposed in this section to assess the winding types to provide a comprehensive view to design machines for the context of HDEV applications. From previous discussions, there is negligible difference between, (i) OLPW and NOLPW, (ii) star and delta, and (iii) lap and concentric. Therefore, these are not considered in the evaluation system for this section.

The output parameters considered are torque density, power density, torque per volt, efficiency, peak temperature, and torque ripple, in descending order of importance. These are given weighting factors, based on the most important to least important order, but also based on the magnitude of the difference i.e., efficiency is important, but the range of values is low, so the weighting factor is large, power density is important, and the range is large, so the weighting factor is reduced. Table XI shows the weights assigned for each characteristic.

TABLE XI. Characteristic Weighting Factors

	T. dens (Nm/kg)	*P. dens (kW/kg)*	*TPV (Nm/V)*	*Eff. (%)*	*Temp (°C)*	*T. rip (%)*
Importance	High	High	Medium	Medium	Medium	Low
Range	Medium	High	High	Low	High	Medium
Weight	2	1.5	1.5	2	0.5	0.5

This weighting factor is then multiplied by the percentage difference between the compared topologies, which produces the scores in Table XII for the remaining topologies, with the largest total having the greatest measured impact. Table XII indicates that the most significant changes were seen when altering pitch length and number of layers and the least significant changes that are worth investigation was direct changing of the wire shape without further modification.

VII. Conclusion

Winding topologies are critical in the design of electrical machines but rarely studied for HDEV. This paper provides a comprehensive view of the optimised machine topology within the context of HDEV using a baseline machine, including electromagnetic, thermal, and manufacturing performance.

A quantity comparison criterion was established to evaluate the discussed winding topologies for the HDEV application, and the results show that layer number is the most critical factor that should be considered during the machine design stage, as well as the pitch. Table XII indicates summarises the score and shows that slot parameters had the most significant impacts on the machine performance, as well as input connection parameters such as parallel path, of the parameters considered and for the HDEV automotive application. The evaluation system also provides a general guideline for factors to be scored during the machine stage in other applications, such as automotives. Using the process from **Error! Reference source not found.** and the information in Table XII, a similar process can be used to incorporate the mechanical and manufacture factors.

The evaluation system can be used to support future work considering to combine various winding characteristics to assess combinational topologies. Future work will consider the impact of combinations of various winding characteristics, to see if trends hold and to develop an optimized winding design for the HDEV context.

TABLE XII. Weighted Characteristic Scores

Top.	*T. dens (Nm/kg)*	*P. dens (kW/kg)*	*TPV (Nm/V)*	*Eff. (%)*	*Temp (°C)*	*T. rip (%)*	*Total*
Lay.	30.47	52.49	24.60	0.29	24.23	18.86	198.70
Pitch	2.55	59.91	39.95	1.67	63.94	18.65	199.53
SPP	29.95	2.62	1.92	0.99	9.50	32.57	89.72
Wire type	16.08	16.13	3.44	1.51	35.21	12.52	88.40
Paths	29.82	20.85	19.55	0.84	60.24	29.97	167.03

VIII. REFERENCES

[1] J. G. Isabella Burch, "Survey of Global Activity to Phase Out Internal Combustion Engine Vehicles," in "Survey on Global activities," Climate Center, San Fransisco, March 2020 2020. Accessed: 11/03/2022. [Online]. Available: https://theclimatecenter.org/wp-content/uploads/2020/03/Survey-on-Global-Activities-to-Phase-Out-ICE-Vehicles-update-3.18.20-1.pdf

[2] M. Al-ani *et al.*, "Design of Rare-Earth-Free PM-assisted Synchronous Reluctance Machine for Heavy-duty Automotive Application," *IET Conference Proceedings*, pp. 796-802. [Online]. Available: https://digital-library.theiet.org/content/conferences/10.1049/icp.2021.1193

[3] S. Sripad and V. Viswanathan, "Performance Metrics Required of Next-Generation Batteries to Make a Practical Electric Semi Truck," *ACS Energy Letters*, vol. 2, no. 7, pp. 1669-1673, 2017/07/14 2017, doi: 10.1021/acsenergylett.7b00432.

[4] K. S. Cha, J. W. Chin, S. H. Park, Y. H. Jung, E. C. Lee, and M. S. Lim, "Design Method for Reducing AC Resistance of Traction Motor Using High Fill Factor Coil to Improve the Fuel Economy of eBus," *IEEE/ASME Transactions on Mechatronics*, vol. 26, no. 3, pp. 1260-1270, 2021, doi: 10.1109/TMECH.2021.3054798.

[5] D. Ivliev, V. Kosenkov, O. Vynakov, E. Savolova, and V. Yarmolovych, "Design of a direct current motor with a windingless rotor for electric vehicles," *Eastern-European Journal of Enterprise Technologies*, vol. 4, pp. 41-50, 08/31 2021, doi: 10.15587/1729-4061.2021.231733.

[6] A. P. C. UK, "Towards 2040: A guide to automotive propulsion technologies," in "The roadmap report," Advanced Propulsion Centre UK UK, 26-06-2018 2018. [Online]. Available: https://apcuk.co.uk/app/uploads/2021/09/roadmap-report-26-6-18.pdf

[7] F. Khan, "A novel wound field flux switching machine with salient pole rotor and
nonoverlapping windings," *Turkish Journal of Electrical Engineering & Computer Sciences*, vol. 25, no. 1, 1, p. 14, 2017.

[8] Y. Li, Z. Zhu, X. Wu, A. S. Thomas, and Z. Wu, "Comparative Study of Modular Dual 3-Phase Permanent Magnet Machines With Overlapping/Non-overlapping Windings," *IEEE Transactions on Industry Applications*, vol. 55, no. 4, pp. 3566-3576, 2019, doi: 10.1109/TIA.2019.2908138.

[9] Z. Wen *et al.*, "Modular Power Sharing Control for Bearingless Multi-Three Phase Permanent Magnet Synchronous Machine," *IEEE Transactions on Industrial Electronics*, pp. 1-1, 2021, doi: 10.1109/TIE.2021.3097610.

[10] F. Libert and J. Soulard, "Investigation on Pole-Slot Combinations for Permanent-Magnet Machines with Concentrated Windings," 01/01 2004.

[11] M. A. Kabir and I. Husain, "New multilayer winding configuration for distributed MMF in AC machines with shorter end-turn length," in *2016 IEEE Power and Energy Society General Meeting (PESGM)*, 17-21 July 2016 2016, pp. 1-5, doi: 10.1109/PESGM.2016.7741756.

[12] J. J. Germishuizen and M. J. Kamper, "Classification of symmetrical non-overlapping three-phase windings," in *The XIX International Conference on Electrical Machines - ICEM 2010*, 6-8 Sept. 2010 2010, pp. 1-6, doi: 10.1109/ICELMACH.2010.5608096.

[13] L. Mingda, L. Yingjie, D. Hao, and B. Sarlioglu, "Thermal management and cooling of windings in electrical machines for electric vehicle and traction application," in *2017 IEEE Transportation Electrification Conference and Expo (ITEC)*, 22-24 June 2017 2017, pp. 668-673, doi: 10.1109/ITEC.2017.7993349.

[14] Z. Xiaokun, K. Baoquan, Z. Yuansheng, and X. Feng, "Comparison of Negative-salient Permanent Magnet Synchronous Machines with Concentrated and Distributed Stator Windings," in *2019 22nd International Conference on Electrical Machines and Systems (ICEMS)*, 11-14 Aug. 2019 2019, pp. 1-6, doi: 10.1109/ICEMS.2019.8922501.

[15] N. Bianchi, S. Bolognani, M. D. Pre, and G. Grezzani, "Design considerations for fractional-slot winding configurations of synchronous machines," *IEEE Transactions on Industry Applications*, vol. 42, no. 4, pp. 997-1006, 2006, doi: 10.1109/TIA.2006.876070.

[16] F. Momen, K. Rahman, Y. Son, and P. Savagian, "Electrical propulsion system design of Chevrolet Bolt battery electric vehicle," in *2016 IEEE Energy Conversion Congress and Exposition (ECCE)*, 18-22 Sept. 2016 2016, pp. 1-8, doi: 10.1109/ECCE.2016.7855076.

[17] H. Koke, "COMPARATIVE STUDY OF STRANDED AND BAR WINDINGS
IN AN INDUCTION MOTOR FOR AUTOMOTIVE PROPULSION
APPLICATIONS," Master of Applied Science (2017), The department of mechanical engineering
and the school of graduate studies, McMaster University, Hamilton, Ontario, Canada, 2017.

[18] X. Fan, D. Li, R. Qu, C. Wang, and J. Li, "Hybrid Rectangular Bar Wave Windings to Minimize Winding Losses of Permanent Magnet Machines for EV/HEVs over a Driving Cycle," in *2018 IEEE International Magnetics Conference (INTERMAG)*, 23-27 April 2018 2018, pp. 1-2, doi: 10.1109/INTMAG.2018.8508038.

[19] D. B. Pinhal and D. Gerling, "Driving Cycle Simulation of Wound-Rotor Synchronous Machine with Hairpin Windings Considering AC-Losses," *2019 IEEE Transportation Electrification Conference and Expo (ITEC)*, pp. 1-7, 2019.

[20] G. Venturini, G. Volpe, M. Villani, and M. Popescu, "Investigation of Cooling Solutions for Hairpin Winding in Traction Application," in *2020 International Conference on Electrical Machines (ICEM)*, 23-26 Aug. 2020 2020, vol. 1, pp. 1573-1578, doi: 10.1109/ICEM49940.2020.9271026.

[21] C. R. Sullivan and R. Y. Zhang, "Simplified design method for litz wire," in *2014 IEEE Applied Power Electronics Conference and Exposition - APEC 2014*, 16-20 March 2014 2014, pp. 2667-2674, doi: 10.1109/APEC.2014.6803681.

[22] K. Niyomsatian, J. Gyselinck, and R. V. Sabariego, "New closed-form proximity-effect complex permeability expression for characterizing litz-wire windings," in *Tenth International Conference on Computational Electromagnetics (CEM 2019)*, 19-20 June 2019 2019, pp. 1-2, doi: 10.1049/cp.2019.0117.

[23] M. H. Tavakoli, A. Ojaghi, E. Mohammadi-Manesh, and M. Mansour, "Influence of coil geometry on the induction heating process in crystal growth systems," *Journal of Crystal Growth*, vol. 311, no. 6, pp. 1594-1599, 2009/03/01/ 2009, doi: https://doi.org/10.1016/j.jcrysgro.2009.01.092.

[24] S. M. madani, T. A. Lipo, C. E. Nino, and D. Lugo, "Modeling of a radial permanent magnet motor with trapezoidal shaped poles," in *IEEE International Conference on Electric Machines and Drives, 2005.*, 15-15 May 2005 2005, pp. 1715-1719, doi: 10.1109/IEMDC.2005.195951.

[25] A. Walker, M. Galea, C. Gerada, A. Mebarki, and D. Gerada, "Design considerations for high performance traction machines: Aiming for the FreedomCar 2020 targets," in *2015 International Conference on Electrical Systems for Aircraft, Railway, Ship Propulsion and Road Vehicles (ESARS)*, 3-5 March 2015 2015, pp. 1-6, doi: 10.1109/ESARS.2015.7101451.

[26] B. Lehner and D. Gerling, "Design and comparison of concentrated and distributed winding synchronous reluctance machines," in *2016 IEEE Energy Conversion Congress and Exposition (ECCE)*, 18-22 Sept. 2016 2016, pp. 1-8, doi: 10.1109/ECCE.2016.7855004.

[27] H. Polinder, M. J. Hoeijmakers, and M. Scuotto, "Eddy-current losses in the solid back-iron of permanent-magnet machines with concentrated fractional pitch windings," *IET Conference Proceedings*, pp. 479-483. [Online]. Available: https://digital-library.theiet.org/content/conferences/10.1049/cp_20060155

[28] A. S. Abdel-Khalik, M. A. Elgenedy, S. Ahmed, and A. M. Massoud, "An Improved Fault-Tolerant Five-Phase Induction Machine Using a Combined Star/Pentagon Single Layer Stator Winding Connection," *IEEE Transactions on Industrial Electronics*, vol. 63, no. 1, pp. 618-628, 2016, doi: 10.1109/TIE.2015.2426672.

[29] S. M. Raziee, O. Misir, and B. Ponick, "Combined Star-Delta Winding Analysis," *IEEE Transactions on Energy Conversion*, vol. 33, no. 1, pp. 383-394, 2018, doi: 10.1109/TEC.2017.2742022.

[30] J. Li, D. Choi, and Y. Cho, "Analysis of Rotor Eccentricity in Switched Reluctance Motor With Parallel Winding Using FEM," *IEEE Transactions on Magnetics*, vol. 45, no. 6, pp. 2851-2854, 2009, doi: 10.1109/TMAG.2009.2018694.

[31] N. Bianchi and G. Berardi, "Analytical Approach to Design Hairpin Windings in High Performance Electric Vehicle Motors," in *2018 IEEE Energy Conversion Congress and Exposition (ECCE)*, 23-27 Sept. 2018 2018, pp. 4398-4405, doi: 10.1109/ECCE.2018.8558383.

[32] S. Xue, M. Michon, M. Popescu, and G. Volpe, "Optimisation of Hairpin Winding in Electric Traction Motor Applications," in *2021 IEEE International Electric Machines & Drives Conference (IEMDC)*, 17-20 May 2021 2021, pp. 1-7, doi: 10.1109/IEMDC47953.2021.9449605.